

# We are IntechOpen, the world's leading publisher of Open Access books Built by scientists, for scientists

6,900

Open access books available

185,000

International authors and editors

200M

Downloads

Our authors are among the

154

Countries delivered to

TOP 1%

most cited scientists

12.2%

Contributors from top 500 universities



WEB OF SCIENCE™

Selection of our books indexed in the Book Citation Index  
in Web of Science™ Core Collection (BKCI)

Interested in publishing with us?  
Contact [book.department@intechopen.com](mailto:book.department@intechopen.com)

Numbers displayed above are based on latest data collected.  
For more information visit [www.intechopen.com](http://www.intechopen.com)



# The Recent Advances in Magnetorheological Fluids-Based Applications

*Shahin Zareie and Abolghassem Zabihollah*

## Abstract

The magnetorheological fluids (MRF) are a generation of smart fluids with the ability to alter their variable viscosity. Moreover, the state of the MRF can be switched from the semisolid to the fluid phase and vice versa upon applying or removing the magnetic field. The fast response and the controllability are the main features of the MRF-based systems, which make them suitable for applications with high sensitivity and controllability requirements. Nowadays, MRF-based systems are rapidly growing and widely being used in many industries such as civil, aerospace, and automotive. This study presents a comprehensive review to investigate the fundamentals of MRF and manufacturing and applications of MRF-based systems. According to the existing works and current and future demands for MRF-based systems, the trend for future research in this field is recommended.

**Keywords:** magnetorheological fluids, variable viscosity, civil, aerospace, automotive, MRF-based systems, applications

## 1. Introduction

The magnetorheological fluids (MRF) are a generation of smart fluids with the ability to alter their viscosity. Moreover, the state of the MRF can be switched from the semisolid to the fluid phase and vice versa upon applying or removing the magnetic field. The fast response and the controllability are the main features of the MRF-based systems, which make them suitable for applications with high sensitivity and controllability requirements. MRF-based systems are rapidly growing and widely being used in many industries such as civil, aerospace, and automotive. This chapter tends to review the fundamental concepts followed by the most recent developments in MRF-based systems. The discovery of magnetorheological fluid (MRF) goes back to 70 years ago by Rabinov [1] at the US National Bureau of Standards. Since then, hundreds of patents and research articles have been published every year.

MRF is a fluid composed of a carrier fluid, such as silicone oil and iron particles, which are dispersed in the fluid [2, 3], with an ability to alter its basic characteristics and viscosity, when subjected to the magnetic field. [4]. Upon applying a magnetic field, the tiny polarizable particles in MRF make chains between two poles, as shown in **Figure 1** [6]. The chains resist movement up to a certain breaking point (yielding point), which is a function of the strength of the magnetic field [6, 7].

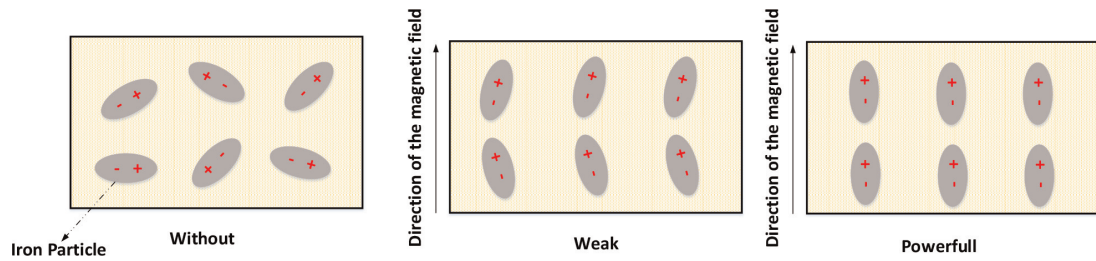


**Figure 1.**  
The effect of magnetic field on polarization of MRFs [5].

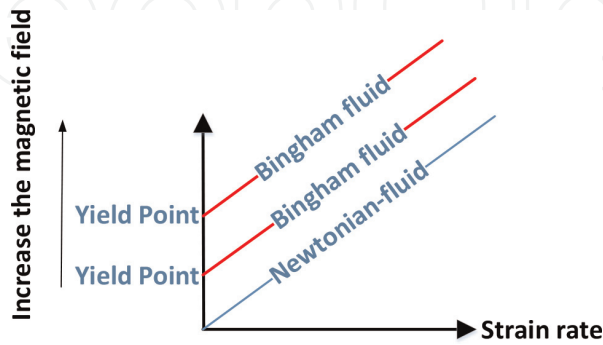


**Figure 2.**  
The relation between shear stress and strain rate of Bingham fluid and Newtonian fluid [8].

In other words, the response of MRF is similar to non-Newtonian fluids, as shown in **Figure 2**.

## 2. Modeling and operational modes of MRF systems

The behavior of MRF may be described by the Bingham plasticity model [1, 2]. The model is expressed by:

$$\tau < \tau_{yield} \rightarrow \dot{\gamma} = 0 \tag{1}$$

$$\tau \geq \tau_{yield} \rightarrow \tau = \tau_{yield} \operatorname{sgn}(\dot{\gamma}) + \mu \dot{\gamma} \tag{2}$$

where  $\tau_{yield}$ ,  $\tau$ ,  $\dot{\gamma}$ , and  $\mu$  are the yielding stress, the shear stress, the strain rate, and the viscosity, respectively [1].

MRF systems operate in three basic modes, valve mode, shear mode, and squeeze mode, as shown in **Figure 3**.

In the following subsection, a brief description of each mode is provided.

### 2.1 MRF flow mode

The flow mode is the most common operational mode of MRF. **Figure 4** shows a simplified geometry of the flow mode. In order to obtain an in-depth understanding

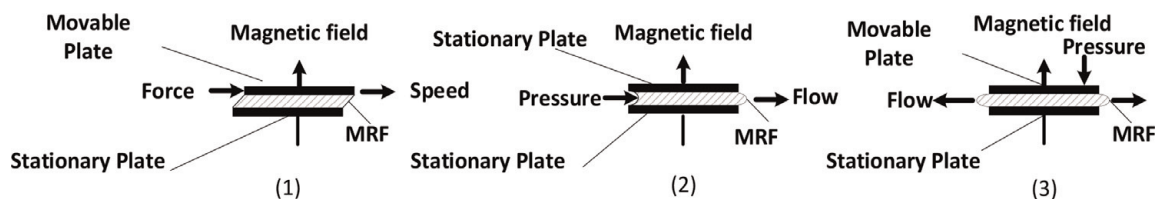


**Figure 3.**  
The operation modes: (1) flow mode, (2) direct shear mode, (3) squeeze mode [9].

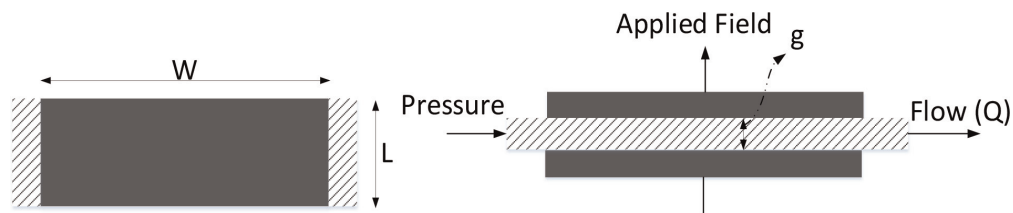


**Figure 4.**  
 The valve mode of MRF [10].

of the damping pressure supplied by MRF in this mode, one may relate the pressure due to the fluid viscosity ( $P_\tau$ ) and the controllable pressure ( $P_\eta$ ).

The total damping pressure can be calculated by [10]:

$$P = P_\eta + P_\tau \quad (3)$$

where  $P_\tau$  and  $P_\eta$  for a Newtonian fluid are expressed by [10]:

$$P_\eta = \left( \frac{12Q\eta L}{wg^3} \right) P_\tau = \frac{C \tau_y L}{g} \quad (4)$$

where  $L$  and  $w$  denote the length and width of parallel plates, respectively. The term  $g$  is the gap between two plates.  $\eta$  and  $Q$  are the plastic viscosity and the fluid flow, correspondingly.  $C$  is a constant value and  $\tau_y$  is the field-dependent yield stress.

### 2.1.1 MRF shear mode

The total amount of force in the shear mode between the two plates (as illustrated in **Figure 5**) is computed by [10]:

$$F = F_\eta + F_\tau \quad (5)$$

where the viscous shear force,  $F_\eta$ , and magnetic-dependent shear force, ( $F_\tau$ ), are represented by [10]:

$$F_\eta = \frac{\eta SA}{g}, \quad F_\tau = \tau_y LW \quad (6)$$

where  $g$ ,  $A$ ,  $S$ , and  $\eta$  indicate the gap between the two plates, the area of the plate, and the relative velocity between the plates, respectively.  $\tau_y$ ,  $L$ , and  $W$  denote the field-dependent yield stress and the width and length of the upper plate.

## 2.2 MRF squeeze mode

The squeeze mode occurs in two cases: compression and tension. In this study, the compressive mode of the MRF between the two plates is considered, and as a

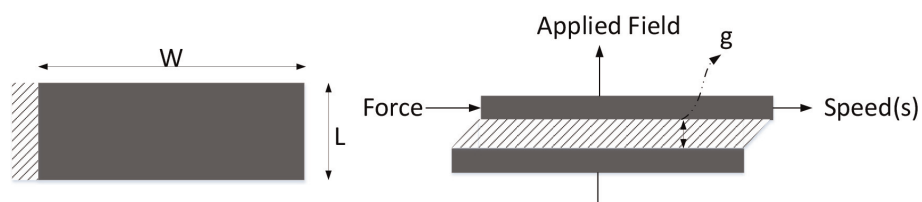


**Figure 5.**  
 The shear mode of MRF [1].

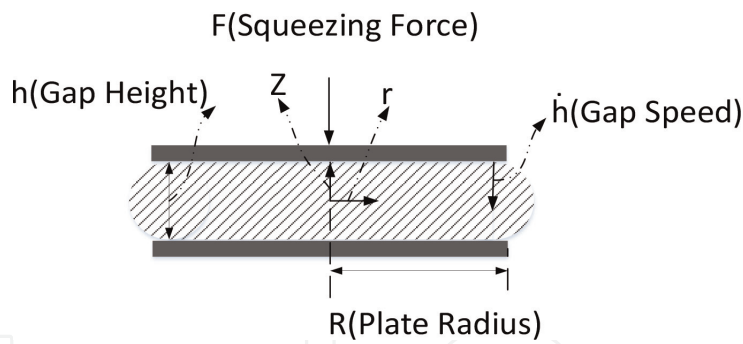


**Figure 6.**  
The squeeze mode of the MRF [1].

result, the fluid moves between the plates as displayed in **Figure 6** [11]. The total amount of force in the squeeze mode is estimated by [11]:

$$F_s = \frac{-\pi R^4}{4} \left( \frac{6\mu\dot{h}}{h^3} + \frac{3\rho\ddot{h}}{5h} - \frac{15\rho\dot{h}^2}{14h^2} \right) \quad (7)$$

where  $R$ ,  $h$ ,  $\mu$ ,  $\ddot{h}$ ,  $\dot{h}$ , and  $\rho$  are the plate radius, the distance between the two parallel plates, the viscosity of the MRF, the gap acceleration, the gap speed, and the density of the MRF, respectively.

### 3. MRF-based applications

Based on MRF characteristics, many devices have been developed. A summary of MRF-based devices is presented in **Figure 7**.

#### 3.1 MRF dampers

MRF devices exhibit outstanding properties, including the large force capacity, the low voltage and the low electric current requirement, fast response, the simple interaction between the electrical current, the damping force, the adaptive rheological properties, the high viscous damping coefficient, easy controllability, and

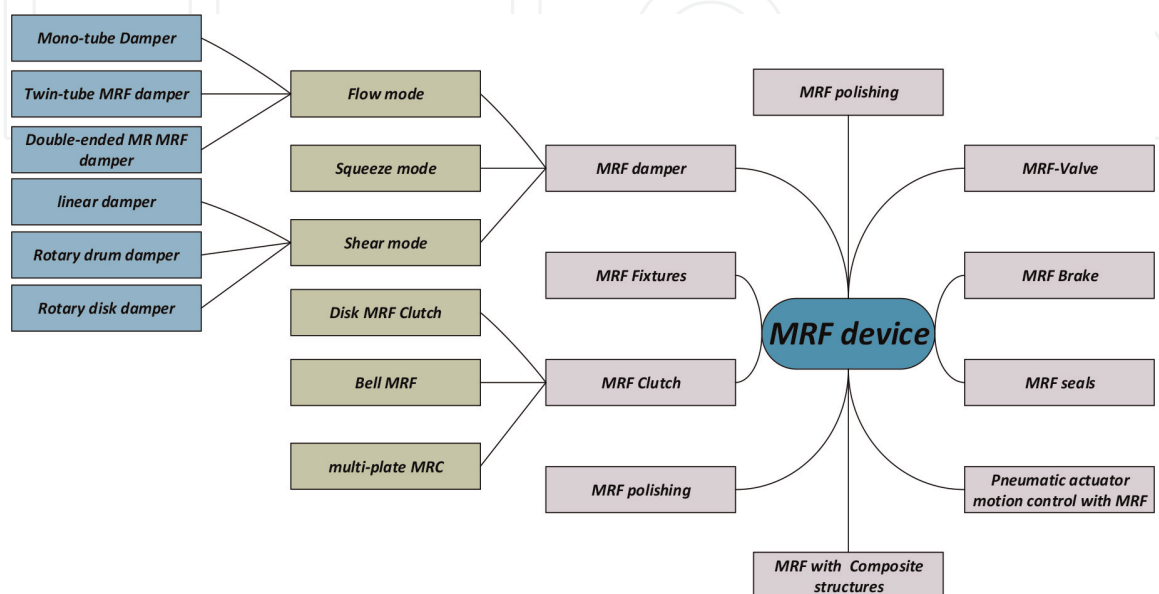


**Figure 7.**  
The summary of MRF devices.

adaptive damping [12–16, 17–21]. MRF dampers are being used widely in the aerospace industry [22], seismic protection [2, 23], and vehicle suspension systems [24]. The core idea of designing simplified MRF dampers derived from hydraulic cylinder damper structures [10, 25]. MRF dampers have been developed based on the three basic operational modes of MRF systems.

### 3.1.1 MRF damper in flow mode

The most common MRF dampers are the mono-tube, the twin-tube, and the double-ended, as represented in **Figures 8–10**, respectively [26, 27]. The working principle of the mono-tube MRF damper as illustrated in **Figure 8** is based on storing pressurized gas in an accumulator located at the bottom of the damper.

**Figure 9** schematically shows the working principles of a twin-tube MRF damper. The outer and inner cylinders are separated by two channels holding pressurized gas. The outer cylinder acts as an accumulator. Contrast to the mono-tube MRF damper, there are two valves: the control valve and foot valve. The function of the foot valve is to control the flow of oil to pass into the gas chamber or to extract the oil from the accumulator [10, 25, 28].

**Figure 10** depicts the double-ended MRF damper, which is derived from the mono-tube MRF damper [10, 29, 30]. Two equal diameter rods are connected from the ends of the housing to the piston. It is worth noting that in double-ended MRF

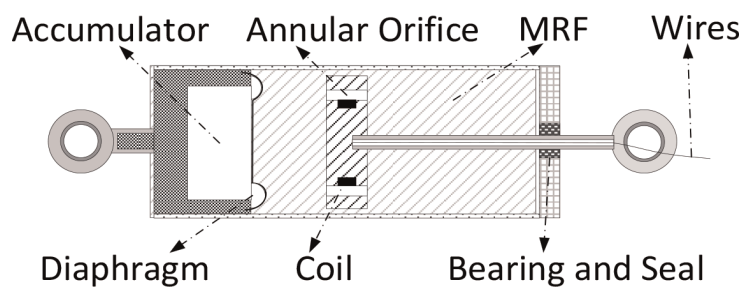


**Figure 8.**  
 Schematic diagram of mono-tube MRF damper [9].

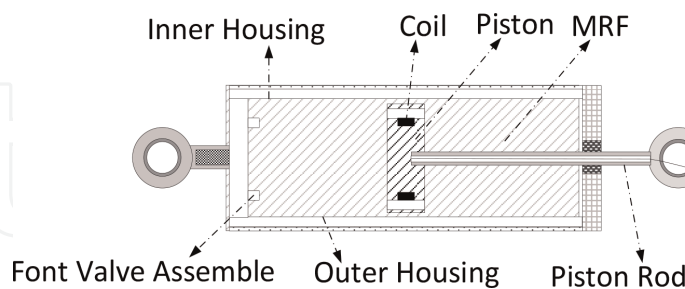


**Figure 9.**  
 Schematic diagram of the twin-tube MRF damper [9].

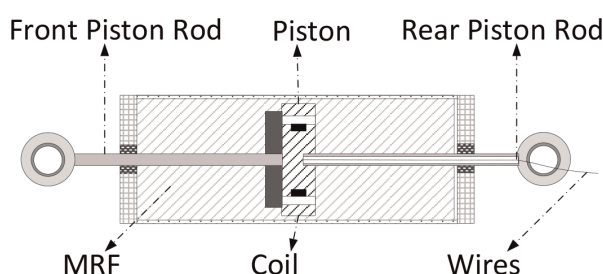


**Figure 10.**  
 Schematic diagram of the double-ended MR MRF damper [9].

damper, the accumulator is not required as long as the volume in the cylinder remains constant while the piston and rod are moving. However, sometimes a small accumulator is used for thermal expansion [30, 31].

### 3.1.2 MRF dampers in shear mode

Shear mode-based dampers are less common than flow mode dampers [32]. They are mostly used to damp rotational vibration. Similar to the flow mode-based MRF damper, these types of dampers work as a passive system in the absence of the magnetic field. The system can be categorized into translational linear motion, rotational disk motion, and rotational drum motion [32].

### 3.1.3 Linear damper

**Figure 11** illustrates a linear shear mode damper which is composed of two parallel plates: a fixed plate at the bottom and a moving one at the top. The two plates are separated by a layer of MRF with thickness  $d$  [32]. The linear force ( $F$ ) between the two plates can be approximated by:

$$F = \tau Lb \quad (8)$$

where  $\tau$ ,  $L$ , and  $b$  are the shear stress, length, and width, respectively.

### 3.1.4 Rotary drum damper

The schematic diagram of a rotary drum damper is shown in **Figure 12**. The system is made of two concentric cylinders where the outer cylinder is held stationary and the inner cylinder rotates [32].

The damping torque ( $T$ ) is computed by [32]:

$$T = 2\pi r^2 L \tau_{r\theta} \quad (9)$$

where  $L$ ,  $r$ , and  $\tau_{r\theta}$  are the cylinder length, the radius coordinate, and the shear stress tensor, respectively.

### 3.1.5 Rotary disk damper

A diagram of a rotary disk damper is shown in **Figure 13** which is composed of two disks: a fixed disk at the bottom and a rotating one at the top. The required torque to rotate the top disk is calculated by [32]:

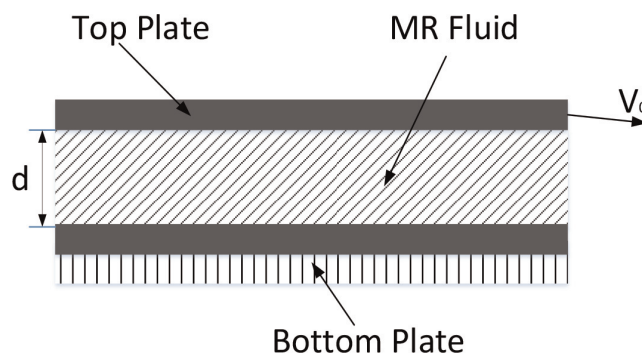


**Figure 11.**  
The linear shear mode damper [32].

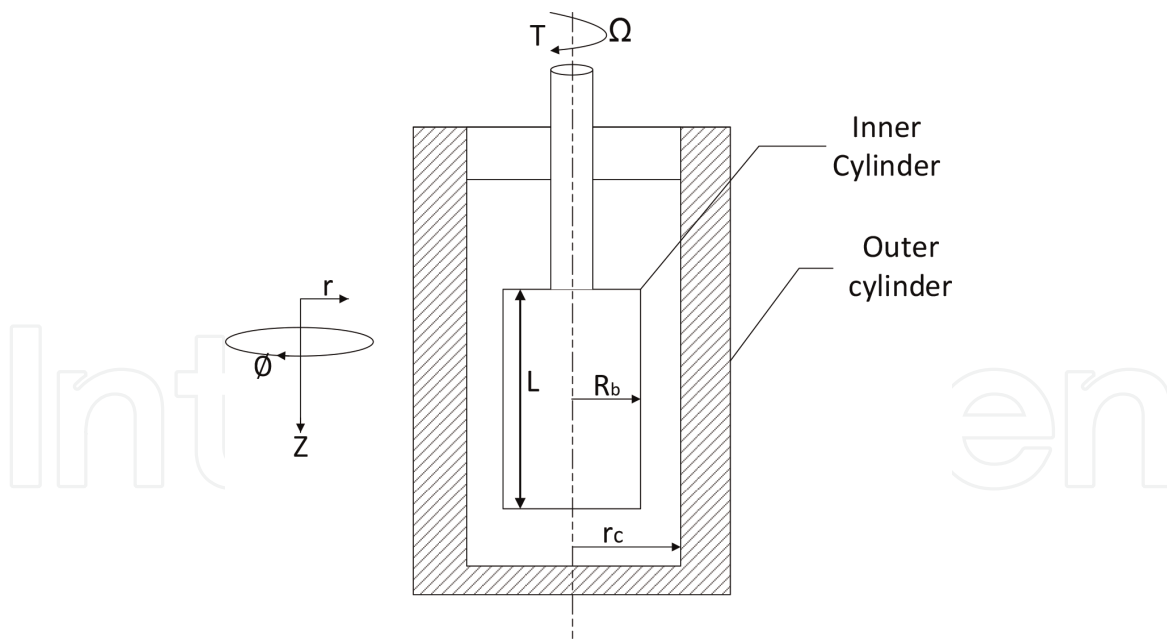


**Figure 12.**  
 The schematic diagram of rotary drum damper [32].

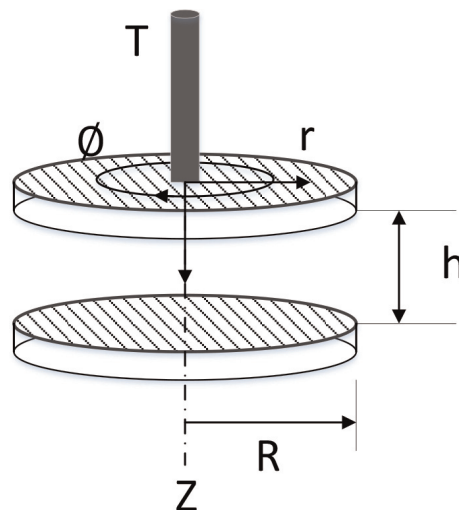


**Figure 13.**  
 The schematic diagram of rotary disk damper [32].

$$T = 2\pi \int_0^R r^2 \tau_{z\theta} dr \quad (10)$$

where  $R$  indicates the radius of the top disk and  $\tau_{z\theta}$  is the shear stress tensor in  $z\theta$  plane.

The MRF damper in the shear mode provides a relative small force. However, the system prevents to form any solidification.

### 3.2 MRF damper in squeeze mode

Recently, due to the large force/displacement ratio, design and development of MRF dampers based on the squeeze mode have been attracted by researchers [17]. **Figure 14** shows the schematic diagram of a damper using the squeeze mode.

In contrast to the flow and the shear mode dampers, the research works in the squeeze mode dampers are very rare [17]. The total force of the top disk is calculated by [17]:

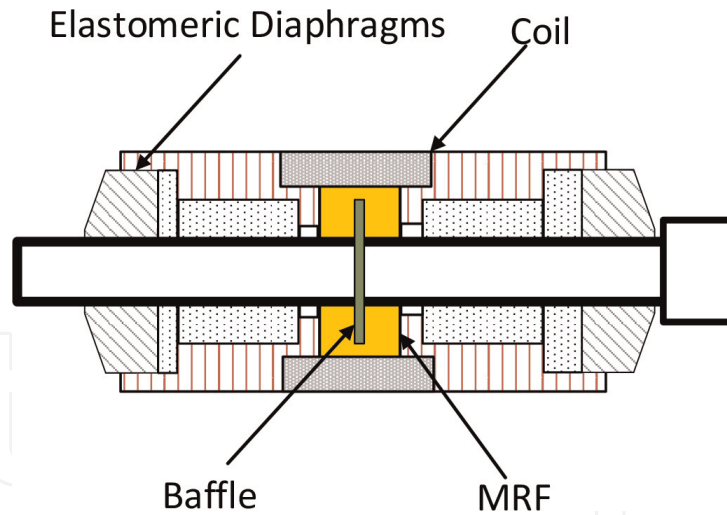


**Figure 14.**  
Schematic diagram of MRF damper in squeeze mode [19].

$$F = 2\pi \int_{R1}^R rp(r)dr \quad (11)$$

where  $r$  and  $p(r)$  are the radius of the cylindrical boundary condition and the total pressure of the upper disk, respectively:

$$p(r) = p_{\eta}(r) + p_{MR}(r) \quad (12)$$

where  $p_{\eta}(r)$  and  $p_{MR}(r)$  indicate the viscous pressure and the pressure considering the MRF effect, respectively. The supplied force is a function of the gap size, the MRF type, and the magnetic field intensity [17]. This damper can generate considerable damping forces while experiencing small displacements. The fundamental behavior of the MRF squeeze mode dampers is not well understood and needs to be more explored. In addition, cavitation effect needs to be considered carefully when designing squeeze mode dampers, as presented in **Table 1** [18].

### 3.3 MRF machining fixtures

Fixtures are important devices to precisely locate the parts during machining [20]. To respond to the demands for holding free-form parts in place efficiently, adaptive or modular fixtures have been developed. Practically, many fixtures may be required to hold all parts in desired locations [20, 21, 33].

Recently, phase-changing materials, such as MRF, become of interest in developing flexible fixtures, due to their fast response and reversibility without temperature change [20]. Due to the very low yield stress of MRF ( $\sim 100$  kPa), the highest clamping forces are obtained in the squeeze mode configuration [20]. **Figures 15** and **16** show two of MRF-based fixtures based on the squeeze mode developed for turbine blades.

### 3.4 MRF clutches

Another important MRF application is intelligent clutches [35, 36] that provide a wide torque transmissibility range upon the applied magnetic field. The long-term

System	Type	Advantages	Disadvantages
MRF damper (flow mode)	Mono-tube damper	Easy to manufacture	Required accumulator, very sensitive to any failure
	Double-ended damper	Less sensitive to failure	Required accumulator, more complex to manufacture
	Twin-tube damper	No accumulator, less sensitive	More complex to manufacture
MRF damper (squeeze mode)		Considerable damping force in small displacement	Possible cavitation, not common
MRF damper (shear mode)		Prevent solidification of MRF	Small relative force (torque)
MRF brake		Rapid response, high torque or force	High cost. Dependent upon rotational speed
MRF clutch	Disk MRC	Wide torque transmissibility range	Homogeneity of the MRF, unpredictable behavior
	Bell MRC	Wide torque transmissibility range	Homogeneity of the MRF, unpredictable behavior
	Multi-plate MRC	Faster response time, less complex, light and compact design	Self-heating, relatively high energy consumption
MRF polishing		Cause to polish surfaces smoothly	Not much effective on hard magnetic materials
MRF valve system		Less friction, fast responses, nonmoving parts, simple electrical circuit	Required extra power
Pneumatic with MRF		Stable and accurate motion control	Required extra power
MRF seals		Simple mechanism, high seal, and low maintenance required	Not effective in high rotary speed
MRF fixture		Fixing irregular-shaped objective	Not common
Composite with MRF		Adaptable damping and stiffness	Added extra weight and required extra power
MRF polishing		Cause to polish surfaces smoothly	Not much effective on hard magnetic materials

**Table 1.**  
 The summary of advantages and disadvantages of MRF-based system.

stability, short reaction time, and good controllability are the main features of MRF clutches [37]. They are promising candidates to be replaced with conventional torque converters and hydraulic starting clutches to enhance the robustness [38].

There are two types of smart clutches as illustrated in **Figure 17**: disk MRF clutches and bell MRF clutches. They are composed of a rotor, a shaft, a coil, MRF, a small gap, and input and output components [35].

In the disk shape clutch, as in all other MRF devices, there are two states: the semisolid state and the liquid state [37]. In the semisolid state, the maximum shear stress is expressed by:

$$\tau_r = \tau_{y,s} \frac{r}{R_0} \quad (13)$$

where  $\tau_{y,s}$ ,  $r$ , and  $R$  are maximum shear stress, the radius of the shaft, and the radius of the disk, respectively.

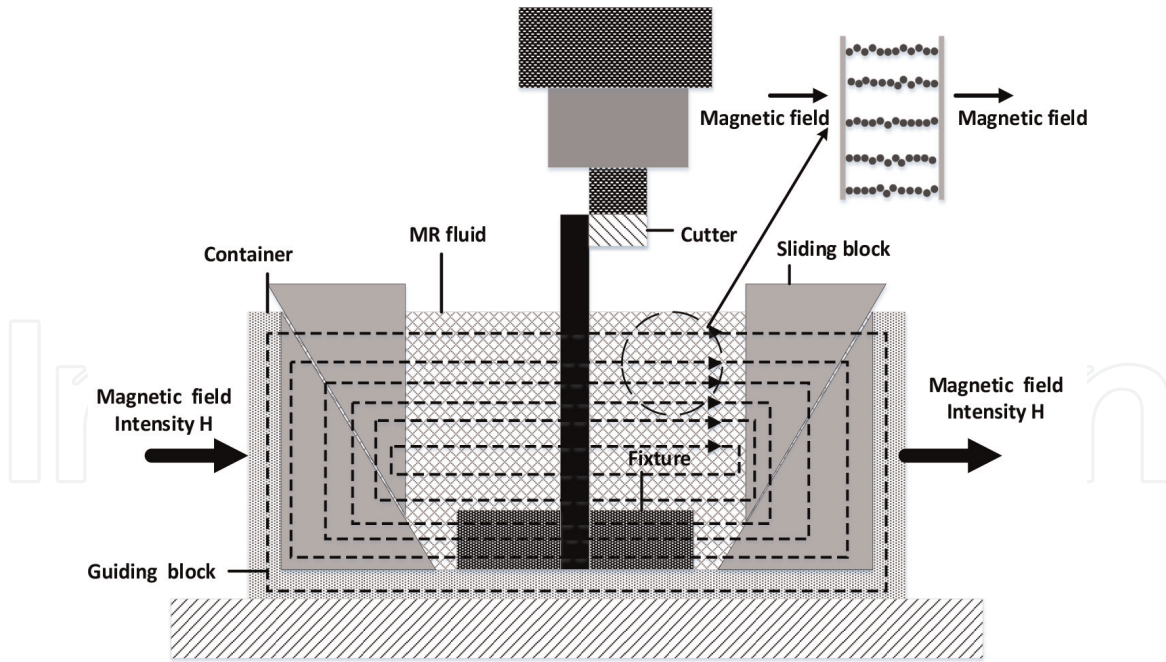


Figure 15.  
The MRF-flexible-fixture prototype [34].

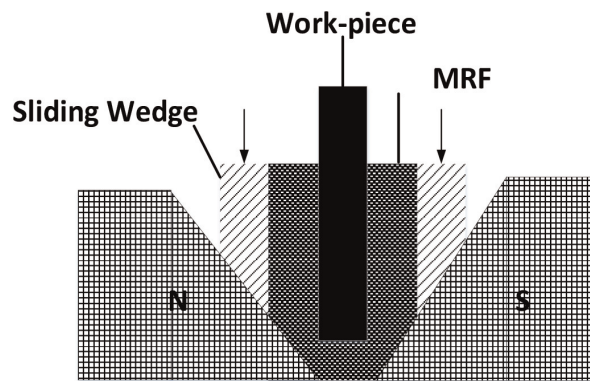


Figure 16.  
The MRF-flexible-fixture prototype [20].

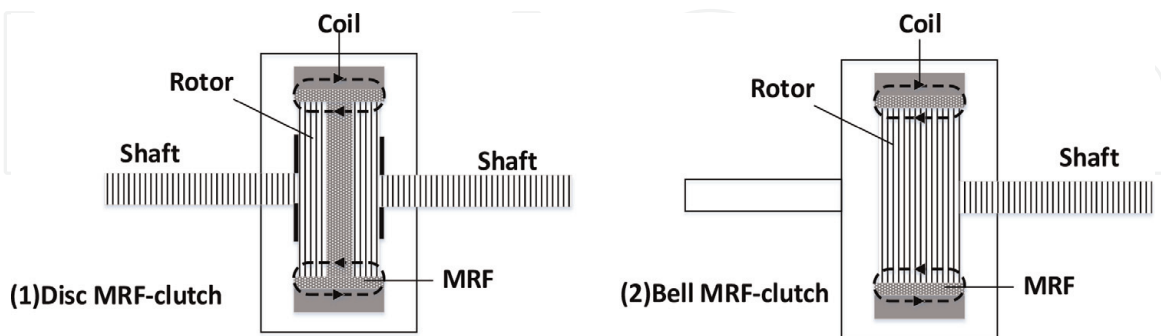


Figure 17.  
Disk and bell MRF clutches [39].

$$T_{\max,S} = \pi\tau_{y,s} \frac{R_0^4 - R^4}{2R_0} \quad (14)$$

In the liquid state, shear stress is computed by:

$$\tau(r) = \tau_{y,d} + \eta(\omega_2 - \omega_1) \left(\frac{r}{s}\right) \quad (15)$$

where  $\tau_{y,d}$ ,  $\eta$ ,  $\omega_2$ , and  $\omega_1$  represent the maximum shear stress, the dynamic viscosity, the angular velocity in disk 2, and angular velocity of disk 1, respectively.

The maximum torque transmitted in the liquid state in a simplified format is determined by:

$$T_{\max,L} = \pi\tau_{y,d} (R_0^3 - R_i^3) \frac{2}{3} \quad (16)$$

In the bell-shaped MRCs, the torque of the semisolid state can be given by:

$$T_{\max,S} = [\pi/(2L\tau_{(y,s)})] (R_i + R_o)^2 \quad (17)$$

where  $L$ ,  $R_0$ , and  $R_i$  are the thickness of MRF, radius of input rotor, and radius of output rotor, respectively.

In the liquid state, torque is described by [37]:

$$T_{\max,L} = [\pi/(2L\tau_{(y,d)})] (R_i + R_o)^2 \quad (18)$$

The major problem in the development of this application is the difference of the density between iron particles and the carrier oil [38]. Micron-sized ferrous particles move outward faster under very high centrifugal forces. Therefore, the homogeneity of the MRF is disturbed leading to an unpredictable behavior MRC [38]. This effect has been studied by many researchers [40, 41]. In order to overcome this problem, a MRF sponge has been introduced to enhance the homogeneity of MRF in the MRC at high speeds [38].

A multi-plate MRC as shown in **Figure 18** has been introduced by Kavlicoglu et al. [42]. It is composed of 43 plates on the rotor to reduce misalignment and distribute the MRF inside the MRC more accurately [42]. Experimental and analytical works proved that the magnitude of the velocity did not affect the performance of the MRC.

The disadvantage of MRF clutches are mainly the high power required to activate the MRF and self-heating while transmitting torque from the drive side to the power off side [35].

Briefly, the comparison between different clutches is conducted and presented. It is observed that both Disk MRC and Bell MRC exhibit a wide range of torque transmissibility. It is worth noting that MRF behavior is unpredictable and the distribution of MRF is not uniform in these systems. However, multi-plate MRC is easy to manufacture, and its response is notably fast.

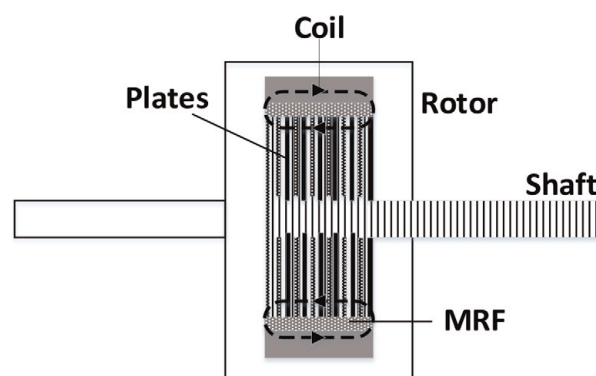


**Figure 18.**  
 Multi-plate MRC [39].

### 3.5 MRF polishing

Another application of MRFs is polishing or finishing based on the magnetic-assisted hydrodynamic polishing [19]. This application can be applied to plastics, optical glasses, ceramics, and complex optical devices, such as spheres. MRF polishing typically provides less surface damage compared to the conventional method [43].

**Figures 19** and **20** depict the operational mechanism of the MRF polishing. As shown, the MRF fills the small gap between the workpiece and the moving wall. The magnetic field changes the viscosity and transforms it into the semisolid state [19]. The moving wall causes a profile of shear stress through the MRF layer resulting in polishing the surface of the work piece [45]. The removal rate ( $R$ ) can be expressed by [43]:

$$R = KPV \quad (19)$$

where  $K$ ,  $P$ , and  $V$  are the Preston coefficient, the pressure, and the velocity between the work piece and the MR fluid and the materials' removal rate, respectively [46].

The positive and negative consequences of the MRF-based polishing systems are shown in **Table 1**. It is found that the system can polish the sensitive surface smoothly. However, the system is not effective for polishing the solid magnetic surface.

### 3.6 MRF valves

One of the novel applications of MRF is the MRF-based valves [47–49], particularly small-size valves [50]. **Figure 21** exhibits the MRF-based valve schematically proposed by Imaduddin et al. [50].

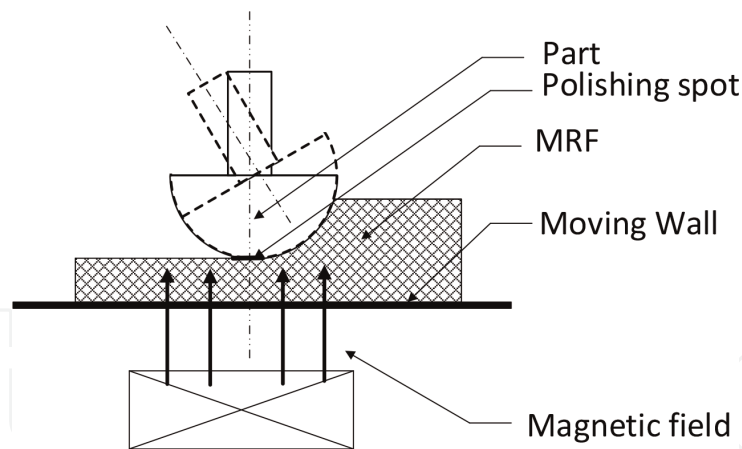


**Figure 19.**  
The schematic diagram of MRF polishing device [44].

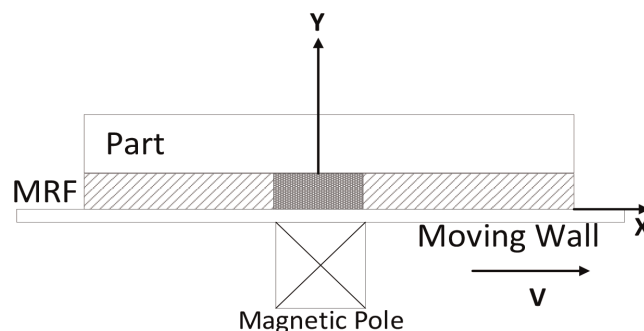


**Figure 20.**  
Schematic working mechanism of MRF polishing [19].

Three structural configurations of MRF valves are annular, radial, and mixed annular and radial gaps [50]. **Figure 21** illustrates a mixed annular and radial gap MRF valve. The pressure drop ( $\Delta p$ ) of the MRF valve is expressed by [50]:

$$\Delta P = \Delta P_{viscous} + \Delta P_{yield} \quad (20)$$

The pressure drop has two parts: the pressure drop ( $p_{viscous}$ ) due to fluid viscosity and pressure drop ( $\Delta p_{yeild}$ ) from field-dependent yield stress [50]. ( $\Delta p_{viscous}$ ) is computed by:

$$\Delta P_{viscous} = \frac{6\eta QL}{\pi R d^3} \quad (21)$$

where  $Q$ ,  $L$ ,  $d$ , and  $R$  represent the base fluid viscosity, the flow rate, the annular channel length of the valve, the valve gaps, and the channel radius, respectively.  $\Delta p_{yeild}$  is computed by:

$$\Delta P_{yeild} = \frac{c\tau(B)L}{d} \quad (22)$$

where the coefficient ( $\tau(B)$ ) represents the field-dependent yield stress value,  $L$  is the annular channel length, and  $d$  is the gap size. The flow-velocity profile  $c$  is written by [50]:

$$c = 2.07 + \frac{12Q\eta}{12Q\eta + 0.8\pi R d^2 \tau(B)} \quad (23)$$

The strengths and weaknesses of the MRF valve system are illustrated in **Table 1**. It is observed that the MRF valves provide fast response, less friction, and simple electrical circuit for actuation.

### 3.7 The MRF brake

MRFs are also used to develop the new type of the braking system and can be replaced with conventional systems. The MRF brake has a high potential to decrease the transmitted torque rapidly subjected to external magnetic fields [51]. In an MRF brake system, the MRF is located between the outer cylinder and the inner rotating cylinder [19]. By energizing solenoid coil, the MRF supplies the resistance shear

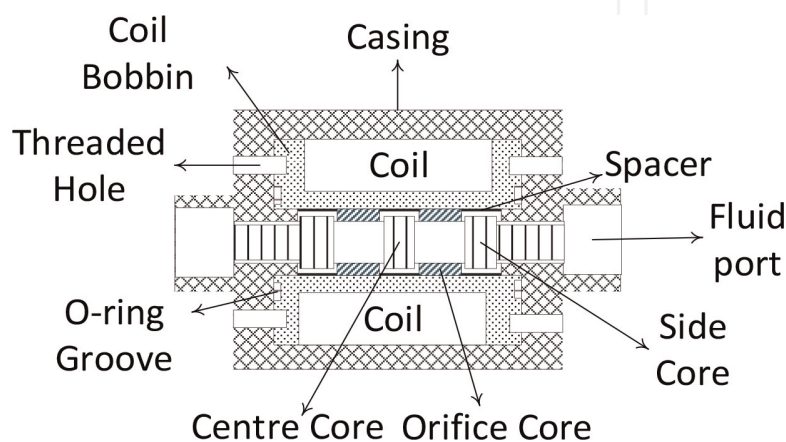


**Figure 21.** Schematic diagram of the MRF valve with annular and radial gaps [50].

force in milliseconds against the torque of the shaft. By removing the magnetic field, the inner cylinder rotates freely [52]. The schematic diagram of the MRF brake is presented in **Figure 22**. The MRF brakes are available in various different shapes, such as drums, disks, and T-shaped rotors [19]. Recently, Sukhwani et al. [53] proposed a new type of the brake based on MR grease. However, their proposed brake provided lower breaking capacity than that of the existing MRF breaks.

The MRF brake system has the capability to supply a huge amount of force (torque).

### 3.8 MRF seals

The sealing of machinery, such as vacuuming equipment, is a significant challenge in the industry [19, 44]. The MRF is considered as a potential technology for sealing pressures up to 3300 kPa [54, 55]. Kanno et al. [54] suggested a one-step seal for a rotary shaft, as illustrated in **Figure 23** schematically. The system was tested at a rotational speed of 1000 rpm with two different sizes of gaps (1–1.7, 0.06–0.5 mm). The major benefits of the system are its ease of operation, good sealing capacity, and low maintenance requirements. Kordonsky et al. [56] studied different intensities of the magnetic fields for different shaft rotation speeds. The study showed that critical pressure is proportionally related to the square of the applied magnetic field strength. Fujita et al. [57] showed that the burst pressure of the seal is a function of size and the volume fraction of MRFs.

As displayed in **Table 1**, the MRF seal needs the external electric power to be actuated, and the performance is not efficient in the rotary movements. However, the working mechanism of MRF seal is simple with a low maintenance.

### 3.9 Pneumatic motion control with the MRF technology

One of the major challenges in pneumatics systems is the accuracy of servo motion control due to the high compression of air, as the working fluid [58]. There are two conventional methods including the airflow regulation and the pneumatic braking for motion control. However, the complexity of these systems is a major challenge. Recently, MRF brakes are being used to enhance the motion control of pneumatic actuators (PAMC), as displayed in **Figure 24** [44]. The system is composed of a pneumatic actuator in parallel with an MRF brake to improve the system performance and functionality due to directional control and complexity of servo

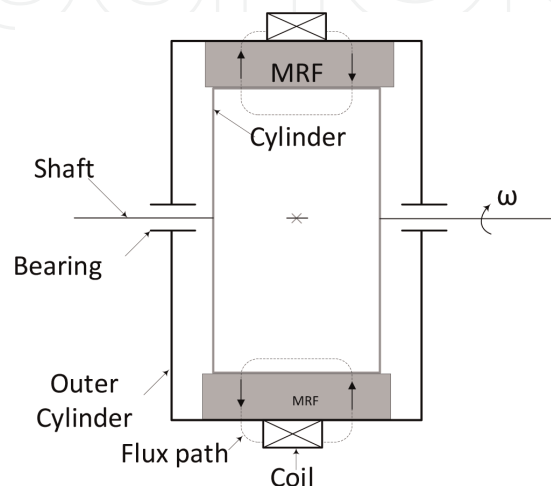


**Figure 22.**  
The typical MRF brake [51].

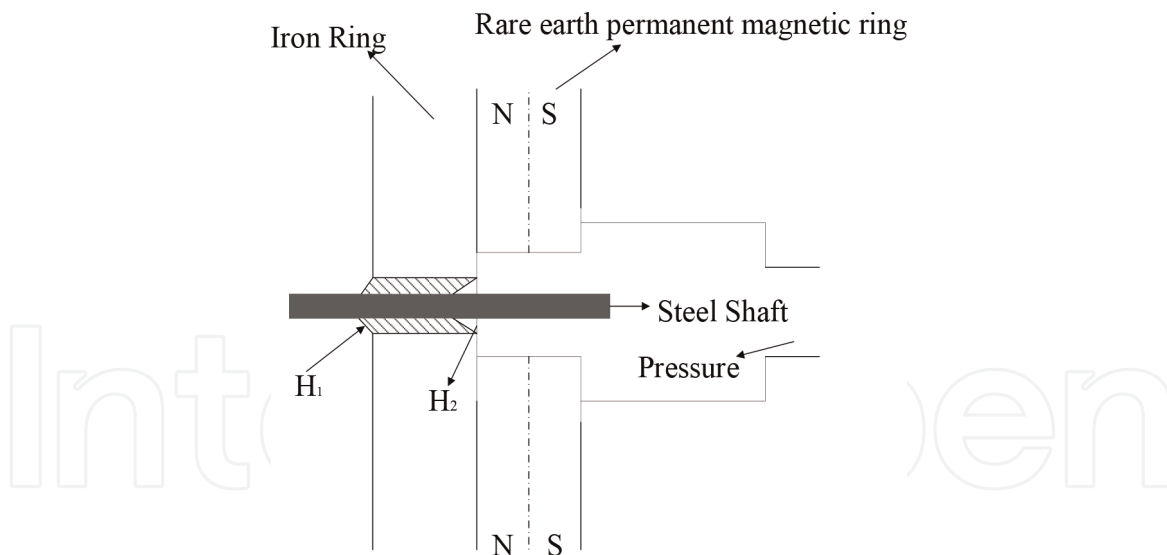


**Figure 23.**  
 Schematic diagram of one-step MRF seal [19].

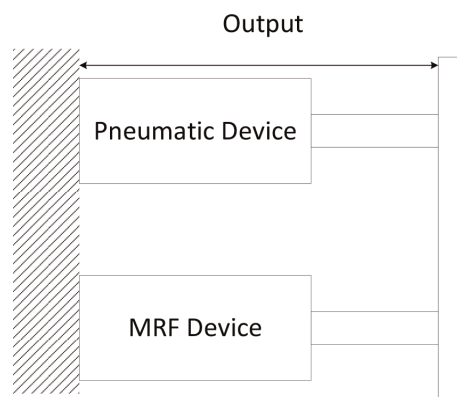


**Figure 24.**  
 Schematic diagram of MRF pneumatic motion control [58].

mechanism [58]. Moreover, the MRF can be used as the pneumatic rotary actuator to control rotary motion and velocities [44, 59–61, 74].

The pneumatic with MRF-based control movement provides higher accuracy. However, the system needs the external power for activation.

### 3.10 MRFs embedded in composite structures

Composite structures are gaining interest in many industries, including civil, transportation, and aerospace due to their excellent mechanical properties, particularly the strength to weight ratio [62–68]. In many applications, the composite structures are exposed to excessive vibration resulting to instability and unpredicted failure. In order to suppress the vibration in composite structures, different methods including passive, semi-active, and active vibration controls have been developed [41, 69–72].

Naji et al. [73] studied the dynamic behavior of a laminate composite beam integrated with an MRF layer, as shown in **Figure 25**. The study showed that magnetic fields in the range of 0–1600 Gauss reduce the maximum displacement and increase the natural frequency. The MRF composite has potential applications in aerospace, civil infrastructures, and automobile industries to suppress the excessive vibrations and/or control the sound propagation, as presented in **Table 1** [69].

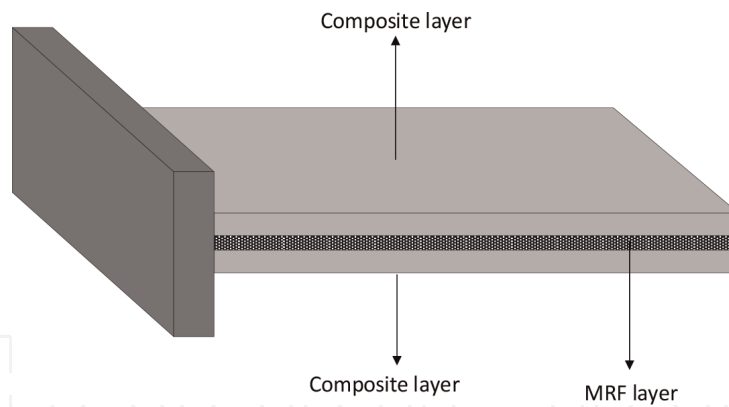


**Figure 25.**  
*Schematic diagram of an adaptive MRF-laminated composite beam [73].*

It is noted that adding MRF to laminated composite structures slightly increases the weight of the element.

#### 4. Chapter summary

In this paper, the basic knowledge of MRF and its spectacular characteristics particularly the switching phases between the semisolid state and fluid state via changing the viscosity of MRF has been concisely discussed.

According to the existing works, MRF has been found to be an excellent candidate to be replaced with the conventional fluid in the fluid-based systems. In brief, MRF-based systems improve the performance and functionality of control systems for many applications, particularly in the followings aspects:

1. Controllability: MRF-based systems provide precise output control due to the variable viscosity of MRF and switching between the semisolid and the fluid phases upon application of the magnetic field.
2. Fast response: reaction of MRF-based systems to the applied magnetic field is in the scale of milliseconds, thus making them suitable candidates to be used for real-time control applications.
3. Extensive applications: MRF-based control systems have found extensive applications in a wide range of industries, including civil, aerospace, and automobiles to enhance the performance and functionality of the systems to achieve the desired outputs.

#### Acknowledgements

Help received from M. Daghighi is much appreciated.

IntechOpen

IntechOpen

### **Author details**

Shahin Zareie\* and Abolghassem Zabihollah  
School of Science and Engineering, Sharif University of Technology,  
International Campus, Iran

\*Address all correspondence to: [zareie\\_shahin@alum.sharif.edu](mailto:zareie_shahin@alum.sharif.edu)

### **IntechOpen**

---

© 2020 The Author(s). Licensee IntechOpen. Distributed under the terms of the Creative Commons Attribution - NonCommercial 4.0 License (<https://creativecommons.org/licenses/by-nc/4.0/>), which permits use, distribution and reproduction for non-commercial purposes, provided the original is properly cited. 

## References

- [1] Rabinow J. Themagnetic fluid clutch. *AIEETrans.* 1948;**67**:1308-1315
- [2] Iqbal MF. Application of magneto-rheological dampers to control dynamic response of buildings. Concordia University; 2009
- [3] Chu SY, Soong TT, Reinhorn AM. Active, Hybrid and Semi-Active Structural Control—A Design and Implementation Handbook. John Wiley & Sons; 2005. ISBN: 978-0-470-01352-6
- [4] Yazid IIM, Mazlan SA, Kikuchi T, Zamzuri H, Imaduddin F. Design of magnetorheological damper with a combination of shear and squeeze modes. *Materials and Design.* 2014;**54**: 87-95
- [5] Sapiński B, Filuś J. Analysis of parametric models of MR linear damper. *Journal of Theoretical and Applied Mechanics.* 2003;**41**(2):215-240
- [6] Esteki K. Developing New Analytical and numerical models for Mr Fluid dampers and their application to seismic design of buildings. The Department of Building, Civil, and Environmental Engineering, Concordia University; 2014
- [7] Yang S, Li S, Wang X, Gordaninejad F, Hitchcock G. A hysteresis model for magneto-rheological damper. *International Journal of Nonlinear Sciences and Numerical Simulation.* 2005;**6**(2):139-144
- [8] Grunwald A. Design and Optimization of Magnetostrictive Actuator. Dublin City University; 2007
- [9] Xiacong Z, Xingjian J, Li C. Magnetorheological fluid dampers: A review on structure design and analysis. *Journal of Intelligent Material Systems and Structures.* 2012;**23**(8):839-873
- [10] Poynor JC. Innovative Designs for Magneto-Rheological Dampers. Virginia Polytechnic Institute and State University. Virginia Tech; 2001
- [11] McIntyre EC. Compression of Smart Materials: Squeeze Flow of Electrorheological and Magnetorheological Fluids. ProQuest; 2008
- [12] Sternberg A, Zemp R, de la Llera JC. Multiphysics behavior of a magneto-rheological damper and experimental validation. *Engineering Structures.* 2014;**69**:194-205
- [13] Luu M, Martinez-Rodrigo MD, Zabel V, Könke C. Semi-active magnetorheological dampers for reducing response of high-speed railway bridges. *Control Engineering Practice.* 2014;**32**:147-160
- [14] Nguyen Q-H, Choi S-B. Optimal design of a vehicle magnetorheological damper considering the damping force and dynamic range. *Smart Materials and Structures.* 2008;**18**(1):15013
- [15] De Vicente J, Klingenberg DJ, Hidalgo-Alvarez R. Magnetorheological fluids: A review. *Soft Matter.* 2011;**7**(8): 3701-3710
- [16] Jiang Z, Christenson R. A comparison of 200 kN magneto-rheological damper models for use in real-time hybrid simulation pretesting. *Smart Materials and Structures.* 2011; **20**(6):65011
- [17] Farjoud A, Cavey R, Ahmadian M, Craft M. Magneto-rheological fluid behavior in squeeze mode. *Smart Materials and Structures.* 2009;**18**(9):95001
- [18] Boelter R, Janocha H. Design rules for MR fluid actuators in different

- working modes. In: *Smart Structures and Materials. Passive Damping and Isolation*. International Society for Optics and Photonics; 9 May, 1997;**3045**: 148-160
- [19] Hajalilou A, Mazlan SA, Lavvafi H, Shameli K. *Magnetorheological Fluid Applications*. In: *Field Responsive Fluids as Smart Materials*. Springer; 2016. pp. 67-81
- [20] Tang X, Zhang X, Tao R. Flexible fixture device with magneto-rheological fluids. *Journal of Intelligent Material Systems and Structures*. 1999;**10**(9): 690-694
- [21] Trappey JC, Liu CR. A literature survey of fixture design automation. *International Journal of Advanced Manufacturing Technology*. 1990;**5**(3): 240-255
- [22] Batterbee DC, Sims ND, Stanway R, Wolejsza Z. Magnetorheological landing gear: 1. A design methodology. *Smart Materials and Structures*. 2007;**16**(6): 2429
- [23] Dominguez A, Sedaghati R, Stiharu I. Modeling and application of MR dampers in semi-adaptive structures. *Computers and Structures*. 2008;**86**(3): 407-415
- [24] Carlson JD. MR fluids and devices in the real world. *International Journal of Modern Physics B*. 2005;**19**(07n09): 1463-1470
- [25] Gillespie T. Development of semi-active damper for heavy off-road military vehicles. *Masters Abstracts International*. 2006; **45**(04)
- [26] Reichert BA. *Application of Magnetorheological Dampers for Vehicle Seat Suspensions*. Virginia Polytechnic Institute and State University. Virginia Tech; 1997
- [27] Ebrahimi B. *Development of Hybrid Electromagnetic Dampers for Vehicle Suspension Systems*. University of Waterloo; 2009
- [28] Goncalves FD. *Characterizing the behavior of magnetorheological fluids at high velocities and high shear rates*. Virginia Polytechnic Institute and State University; 2005
- [29] Norris JA, Ahmadian M. Behavior of magneto-rheological fluids subject to impact and shock loading. In: *ASME 2003 International Mechanical Engineering Congress and Exposition*; 2003. pp. 199-204
- [30] Abu-Ein SQ, Fayyad SM, Momani W, Al-Alawin A, Momani M. Experimental investigation of using MR fluids in automobiles suspension systems. *Research Journal of Applied Sciences, Engineering and Technology*. 2010;**2**(2):159-163
- [31] Wang Q, Ahmadian M, Chen Z. A novel double-piston magnetorheological damper for space truss structures vibration suppression. *Shock and Vibration*. 2014;**2014**
- [32] Wereley NM, Cho JU, Choi YT, Choi SB. Magnetorheological dampers in shear mode. *Smart Materials and Structures*. 2007;**17**(1):15022
- [33] Arzanpour S, Fung J, Mills JK, Cleghorn WL. Flexible fixture design with applications to assembly of sheet metal automotive body parts. *Assembly Automation*. 2006;**26**(2):143-153
- [34] Ma J, Zhang D, Wu B, Luo M, Liu Y. Stability improvement and vibration suppression of the thin-walled workpiece in milling process via magnetorheological fluid flexible fixture. *The International Journal of Advanced Manufacturing Technology*. 1 Feb, 2017;**88**(5-8): 1231-1242

- [35] Jackel M, Kloepfer J, Matthias M, Seipel B. The novel MRF-ball-clutch design a MRF-safety-clutch for high torque applications. *Journal of Physics: Conference Series*. 2013;**412**(1):12051
- [36] Najmaei N, Asadian A, Kermani MR, Patel RV. Magneto-rheological actuators for haptic devices: Design, modeling, control, and validation of a prototype clutch. In: *Robotics and Automation (ICRA), 2015 IEEE International Conference; 2015*. pp. 207-212
- [37] Lampe D, Thess A, Dotzauer C. MRF-clutch-design considerations and performance. *Transition*. 1998;**3**:10
- [38] Neelakantan VA, Washington GN. Modeling and reduction of centrifuging in magnetorheological (MR) transmission clutches for automotive applications. *Journal of Intelligent Material Systems and Structures*. 2005; **16**(9):703-711
- [39] Xu X, Zeng C. Notice of retraction design of a magneto-rheological fluid clutch based on electromagnetic finite element analysis. In: *2nd International Conference on Computer Engineering and Technology*. IEEE; 2010. Vol. 5, pp. V5-182
- [40] Bansbach EA. Torque Transfer Apparatus Using Magnetorheological Fluids. Google Patents, 1998
- [41] Gopalswamy S, Jones GL. Magnetorheological Transmission Clutch. Google Patents; 1998
- [42] Kavlicoglu BM, Gordaninejad F, Evrensel CA, Cobanoglu N, Liu Y, Fuchs A, et al. High-torque magnetorheological fluid clutch. In: *Smart Structures and Materials*. International Society for Optics and Photonics. Damping and Isolation. 27 Jun 2002;**4697**:393-401
- [43] Kordonski W, Golini D. Progress update in magnetorheological finishing. *International Journal of Modern Physics B*. 1999;**13**(14n16):2205-2212
- [44] Wang J, Meng G. Magnetorheological fluid devices: principles, characteristics and applications in mechanical engineering. *Proceedings of the Institution of Mechanical Engineers, Part L: Journal of Materials: Design and Applications*. 2001;**215**(3):165-174
- [45] Jacobs SD. Manipulating mechanics and chemistry in precision optics finishing. *Science and Technology of Advanced Materials*. 2007;**8**(3):153-157
- [46] Jain VK, Sidpara A, Sankar MR, Das M. Nano-finishing techniques: A review. *Proceedings of the Institution of Mechanical Engineers, Part C: Journal of Mechanical Engineering Science*. 2012; **226**(2):327-346
- [47] Manoharan V. Magneto-Rheological Fluid Device as Artificial Feel Force System On Aircraft Control Stick. *Dissertations and Theses*. 2016. Available from: <https://commons.erau.edu/edt/225>
- [48] Muzakkir SM, Hirani H. A magnetorheological fluid based design of variable valve timing system for internal combustion engine using axiomatic design. *International Journal of Current Innovation Research*. 2015; **5**(2):603-612
- [49] Yoo J-H, Wereley NM. Design of a high-efficiency magnetorheological valve. *Journal of Intelligent Material Systems and Structures*. 2002;**13**(10): 679-685
- [50] Imaduddin F, Mazlan SA, Zamzuri H, Yazid II. Design and performance analysis of a compact magnetorheological valve with multiple annular and radial gaps. *Journal of*

Intelligent Material Systems and Structures. Jun 2015;**26**(9):1038-1049

[51] Huang J, Zhang JQ, Yang Y, Wei YQ. Analysis and design of a cylindrical magneto-rheological fluid brake. *Journal of Materials Processing Technology*. 2002;**129**(1):559-562

[52] Huang J, Wang H, Ling J, Wei YQ, Zhang JQ. Research on chain-model of the transmission mechanical property of the magnetorheological fluids. *Mach. Des. Manuf. Eng.* 2001;**30**(2):3-7

[53] Sukhwani VK, Hirani H. A comparative study of magnetorheological-fluid-brake and magnetorheological-grease-brake. *Tribology*. Online. 2008;**3**(1):31-35

[54] Kanno T, Kouda Y, Takeishi Y, Minagawa T, Yamamoto Y. Preparation of magnetic fluid having active-gas resistance and ultra-low vapor pressure for magnetic fluid vacuum seals. *Tribology International*. 1997;**30**(9):701-705

[55] Browne AL, Johnson NL, Barvosa-Carter W, McKnight GP, Keefe AC, Henry CP. Active Material Based Seal Assemblies. Google Patents; 2012

[56] Kordonsky W. Elements and devices based on magnetorheological effect. *Journal of Intelligent Material Systems and Structures*. 1993;**4**(1):65-69

[57] Fujita T, Yoshimura K, Seki Y, Dodbiba G, Miyazaki T, Numakura S. Characterization of magnetorheological suspension for seal. *Journal of Intelligent Material Systems and Structures*. 1999;**10**(10):770-774

[58] Jolly MR. Pneumatic motion control using magnetorheological technology. In: *Smart Structures and Materials. Industrial and Commercial Applications of Smart Structures Technologies*. International Society for Optics and Photonics. 14 Jun 2001;**4332**:300-308

[59] Alam M, Choudhury IA, Bin Mamat A. Mechanism and design analysis of articulated ankle foot orthoses for drop-foot. *The Scientific World Journal*. 2014; **2014**:14. Article ID 867869. Available from: <https://doi.org/10.1155/2014/867869>

[60] Zhu X, Jing X, Cheng L. A magnetorheological fluid embedded pneumatic vibration isolator allowing independently adjustable stiffness and damping. *Smart Materials and Structures*. 2011;**20**(8):85025

[61] Mikułowski GM, Holnicki-Szulc J. Adaptive landing gear concept feedback control validation. *Smart Materials and Structures*. 2007;**16**(6):2146

[62] Zareie S, Zabihollah A. A failure control method for smart composite morphing airfoil by piezoelectric actuator. *Transactions of the Canadian Society for Mechanical Engineering*. 2011;**35**(3):369-381

[63] Hosseiny SA, Jakobsen J. Local fatigue behavior in tapered areas of large offshore wind turbine blades. In: *IOP Conference Series: Materials Science and Engineering*. IOP Publishing; Jul 2016;**139**(1):012022

[64] Pol MH, Zabihollah A, Zareie S, Liaghat G. Effects of nano-particles concentration on dynamic response of laminated nanocomposite beam/Nano daleliu koncentracijos itaka dinaminei nanokompozicinio laminuoto strypo reakcijai. *Mechanika*. 2013;**19**(1):53-58

[65] Fattahi SJ, Zabihollah A, Zareie S. Vibration monitoring of wind turbine blade using fiber bragg grating. *Wind Engineering*. 2010;**34**(6)

[66] Zabihollah A, Momeni S, Ghafari AS. Effects of nanoparticles on the improvement of the dynamic response of nonuniform-thickness laminated

- composite beams. *Journal of Mechanical Science and Technology*. 1 Jun 2016;**30**(1):121-125
- [67] Zabihollah A, Zareie S. Optimal design of adaptive laminated beam using layerwise finite element. *Journal of Sensors*. 2011;**2011**:8. Article ID 240341. Available from: <https://doi.org/10.1155/2011/240341>
- [68] Zareie S, Zabihollah A. A failure control method for smart composite morphing airfoil by piezoelectric actuator. *Transactions of the Canadian Society for Mechanical Engineering*. 2011;**35**(3)
- [69] Manoharan R, Vasudevan R, Jeevanantham AK. Dynamic characterization of a laminated composite magnetorheological fluid sandwich plate. *Smart Materials and Structures*. 2014;**23**(2):25022
- [70] Lim SH, Prusty BG, Pearce G, Kelly D, Thomson RS. Study of magnetorheological fluids towards smart energy absorption of composite structures for crashworthiness. *Mechanics of Advanced Materials and Structures*. 2016;**23**(5):538-544
- [71] Rajamohan V, Rakheja S, Sedaghati R. Vibration analysis of a partially treated multi-layer beam with magnetorheological fluid. *Journal of Sound and Vibration*. 2010;**329**(17):3451-3469
- [72] Zabihollah A, Ghafari AS, Yadegari A, Rashidi D. Effects of MR-fluid on low-velocity impact response of MR-laminated beams. In: *AIP Conference Proceedings*. Vol. 1858, No. 1; 2017. p. 40004
- [73] Naji J, Zabihollah A, Behzad M. Vibration characteristics of laminated composite beams with magnetorheological layer using layerwise theory. *Mechanics of Advanced Materials and Structures*. 2018;**25**(3):202-211. DOI: 10.1080/15376494.2016.1255819
- [74] Lee H-G, Sang-Hyun K-WM, Chung L, Lee S-K, Lee M-K, Hwang J-S, et al. Pneumatic motion control using magnetorheological technology. *Journal of Intelligent Material Systems and Structures*. 2007;**18**(19):1111-1120